Paper No: 03-IAGT-203

15TH SYMPOSIUM ON INDUSTRIAL APPLICATIONS OF GAS TURBINES

EFFECT OF FLOW RATE INCREASE ON POTENTIAL DISK-BLADE FAILURE

by

Roman Motriuk

Of
Arcus Solutions Inc.
Calgary AB

Presented at the 15th Symposium on Industrial Application of Gas Turbines
Banff, Alberta, Canada - October 13 - 17, 2003
The IAGT Committee is sponsored by the Canadian Gas Association.

Biography Session 2.3

Roman Motriuk

Roman W. Motriuk is a senior engineer with Arcus Solutions Inc. He has over 18 years of consulting experience in the troubleshooting of turbo- and reciprocating machinery, gas turbines and compressors. His experience includes stress analysis, pulsation-vibration, environmental noise control, noise silencing, flow investigations (fluid solid interaction and machinery performance), and the resolution of various metering problems (orifice, turbine and ultrasonic meters).

Roman has M.Sc. degree in Drilling Machines from the AGH Technical University of Cracow (1978) and M.Sc. degree in Applied Acoustics from the University of Calgary (1986). He has spent most of his career with Beta Machinery, Nova, TransCanada, and Arcus Solutions Inc. working in his field of expertise. He routinely troubleshoots dynamic problems and actively participates in research and development projects. He has been teaching the Dynamics of Compressor System course at the University of Calgary for the past three years. He has published over thirty scientific papers on vibration, dynamic stress, and turbo-machinery acoustics. He is a chairman of the Calgary Technical Chapter of the ASME-PSD, a member of the ASME PSD Executive Committee (International), and a co-chair of the International Pipeline Conference (IPC) 2004 Organizing Committee. In addition, he is a member of the Fluid – Solid Interaction (FSI) ASME Committee.

ABSTRACT

High pressure stages of power turbines still fail while operating in their design regimes. Failures are in the blade or disk area. These failures could lead to a catastrophic breakdown of the machine when initial damage is not caught in time. The post failure examinations frequently reveal high and low cycle fatigue cracks of the disks, high cycle fatigue in the root blade area, and localized corrosion of the disk web area with some deposits of different elements such as sulphur, etc. Hence, determining true cause of a failure becomes a complex and tedious task for engineering experts. In addition to the above failure signatures one has to recognize the existence of complex dynamic fields (thermal, acoustical, and flow related) which act on the turbine disks and their blades during the operation.

The author believes that in most cases disk and blade failures are the result of high frequency cycle events. In these events a disk with blades is forced into alternating sine wave deflections causing deformation forces that initiate cracks directly or indirectly either in the disks or blades. It is interesting to notice that the majority of the failures occur in up-rated machines. Therefore, the amount of gas flow through the machine must be an important factor in the above failures.

In this paper the blade vibration levels are predicted while the gas flow through the machine is increased. The calculations are based on the interaction of the acoustic wave with the structural modes of the disk-blade and the interaction efficiency of the coupling between the acoustic and structural modes.

NOMENCLATURE

E Young's modulus
f_α modal frequency
$J_{\alpha\alpha}$ joint acceptance
m circumferential pattern or longitudinal mode number
m_α generalized mass
n harmonic blade passing frequency or lateral mode number
$y_\alpha^2(\vec{x})$ mean square response
$(\vec{x})$ position vector on surface of structure
$d\vec{x}$ integration area (same as dA or dS)
$G_p(f_\alpha)$ oscillating pressure power spectral density
wt plate wall thickness
α modal index, (m,n)
β modal index, (r,s)
λ_{mn} frequency parameter
ρ_m blade/plate material density
ν Poisson's ratio
$\psi_\alpha(\vec{x}) = \psi_m(x_{L_1})\phi_n(x_{L_2})$, mode shape function
ζ_α modal damping

INTRODUCTION

The first set of power turbine blade disks is subjected to very complex excitations which result from many types of combustion instabilities. The instabilities increase heat transfer rate in combustor walls and induce vibrations which could cause structural damage to the combustor itself and the downstream structures. This kind of failures is avoided by employing a trial and error process. Such a process is preferred since accurate predictions of the complex flow through the turbine are most difficult, tedious, and expensive.

The flow stability is influenced by many complex variables such as turbulence, acoustics, chemical kinetics, and vibration. The common parameter controlling these variables is the flow rate. It, along with other parameters such as fuel mixture, turbine channel geometry and bluff bodies stabilizing turbulence, governs the flow stability.

Pressure pattern in the turbine casing exists in the forms of non-propagating but oscillating wall pressures, plane wave pressure oscillations, and higher-order acoustic three-dimensional pressure oscillations. Higher order pressure oscillations are the most efficient excitation sources of turbine combustors and bladed disk rotors. This work attempts to offer a simplified approach to relate the flow rate through a turbine to the vibration response of the first stage disk blades. Only, the random flow excitations are considered and a single turbine blade is approximated to a plate 'resting' on the flow conveying channel. The blade root, one edge of the plate, is considered to be fixed. In spite of the above simplifications, the predicted blade vibration results are informative and they reflect the actual values.

ACOUSTIC EXCITATION

There are two types of acoustic waves that can be excited in the turbine casing. One kind, plane waves, exists when the combustion oscillation is less than the first cut-off frequency of the transverse acoustic mode (1, 0), see Figure 1. The second kind, higher order 3-D waves, when the oscillation is above the first cut-off frequency. The mode corresponding to the above 'cut-off' frequency which is closest to that of the excitation frequency, (for example vortex shedding) has the largest part of the total acoustic energy. In an extreme situation, when the 'cut-off' frequency is very close to the excitation frequency, the pressure oscillation in the combustor is such as if a single mode existed.

A change in the flow rate could start vortex shedding. The vortices could excite the cut-off mode of the combustor-turbine interior which corresponds to the shedding frequency that would lead to a single-tone acoustic resonance. Usually, the amplitude of this tone increases proportionally to the flow velocities. The increase could also happen in distinctive steps when a lock-in mechanism is established. In case of a lock-in mechanism, the discussed phenomenon is initiated and sustained by a feedback between the combustor unstable jets, system acoustics, and the vibrating disk/blade rotor system. At certain flows, the jets form vortices that are stronger than usual and pure acoustic tones are produced due to their interaction with the turbine rotor and casing acoustic natural frequencies. When the pressure fluctuation is reflected and transmitted back to the rotor, the differential pressure across the rotor is slightly increased. A positive force results and it generates the rotor vibration which in turn produces new pressure fluctuation reinforcing the instability of the jets. After several such cycles the amplitude of oscillatory motion of the disk is large enough for the lock-in mechanism to be set up.

DISK-BLADE NATURAL MODES OF VIBRATION

In general, a disk type rotor consists of a disk-blade assembly and a shaft whose diameter is several times smaller than the disk-blade diameter. The blades are tight-fit-attached to the disk as seen in Figure 2. While operating, the disk-blade assembly constitutes a single mechanical system where blades can bend much more easily than the disk. If it is assumed that the disk blade is attached to the stationary shaft, the outer perimeter of the disk-blade is free to vibrate. Such a system has infinite number of natural modes but only a few of them are of significance. The lowest modes are the most important. Observing the modes in Figure 3, one can notice that the circumference of the disk is divided into an even number of equal parts. Half of them deflect up and half of them deflect down, in an out-of-plane direction. These parts are determined for a time instant and oscillate with half a vibrational period. This means that deflections along the circumference are such that when the disk perimeter is developed into a straight line, the deflections can be represented by as a sine curve.

While the rotor rotates its vibration modes change slightly, i.e. vibration frequency is increased and the shape is modified. Frequency increases due to the centrifugal force arising from rotation that stiffens the blade-disk system. The stiffening factor, determined empirically for each considered mode, is approximately related hyperbolically to the angular velocity of the impeller. The factor values are greater than unity.

Fatigue failures of such rotors have been observed in industry. The failures happened mostly in blades. The origin of those failures was identified as a resonance phenomenon between the lowest blade natural frequencies of vibration and some multiple of the running speed. Some of these coincidences however did not result in failures while other did.

COINCIDENCE

In many cases, the vibration energy is delivered to the rotor in a quasi harmonic or random manner. In such situations, calculation of the disk-blade response to the flow excitation alone provides sufficient information about the ‘health’ of the stage disk. Determination of a coincidence between the acoustic mode and the structural mode predicts its life. When there is a complete coincidence (simultaneous frequency and wave number match, Figure 4b, the most severe dynamic loading of the disk-blade occurs. The complete coincidence results in high cycle fatigue failure. On the other hand, a partial coincidence (only

frequency or a wave number match, Figure 4c) does not lead to damage. Hence, to qualify the coincidence both the transfer function and the acceptance integral are used.

ANALYSIS – BLADE-CHANNEL MODEL

The disk-blade rotors used in identical turbines failed while the turbines were upgraded to increase their power. Specifically, turbine discharge pressure differential was increased which raised the turbine flow by about 8%. This modification resulted in change of vibration responses of the disk-blade rotor. To evaluate these changes the following analysis was performed. In the first step, a blade of the first turbine stage, as shown in Figures 5 and 6 was represented by a plate. The gas flow was assumed to be parallel to the blade surface. The blade was modelled as a rectangular plate whose only one end, representing the blade root, was fixed. Only a part of the blade was exposed to a flow through the channel, see Figure 6. The channel was assumed to have a rectangular cross section, see Figure 7. The channel dimensions were based on the disk-blade measurements. The blade thickness varied from 0.5 to 6.5 mm, hence average blade thickness was used in the calculations. For modal predictions, the length of the blade was adjusted to include not only the part exposed to the flow but also the 'fir-tree' root area. Four blade mode-shapes and their natural frequencies were predicted and confirmed by the measurements, see Table 1.

Next, the most significant vibratory responses were determined. In predictions, the maximum response of each mode was given by:

$$< y_\alpha{}^2(\underline{x}) >= \frac{AG_p(f_\alpha)\psi_\alpha{}^2(\underline{x})\underline{J}_{\alpha\alpha}(f_\alpha)}{64\pi^3 m_\alpha{}^2 f_\alpha{}^3 \xi_\alpha} \quad (1)$$

It was assumed that the blade was of uniform thickness and the natural frequencies were well separated. Consequently, the cross terms in equation (1) were ignored. Mode shape function and generalized masses were normalized according to Au-Yang [1] and the acceptance values $\underline{J}_{\alpha\alpha}$ were read off the included charts. The following normalization equation was used:

$$\int_A \psi_\alpha(\underline{x})\psi_\beta(\underline{x})d\underline{x} = \delta_{\alpha\beta} \quad (2)$$

For rectangular blade 'resting' at the edges, the normalized mode shape functions in the longitudinal and lateral directions, ψ_m and ϕ_n respectively, were:

$$\psi_m = \sqrt{\frac{2}{L_1}}\sin\frac{m\pi x}{L_1} \quad (3)$$

$$\phi_n = \sqrt{\frac{2}{L_2}}\sin\frac{n\pi x}{L_2} \quad (4)$$

where L_1 and L_2 were the length and width of the flow channel as depicted in Figure 7.

The maximum value of each mode shape function was calculated to be:

$$\psi_{m\max} = \sqrt{\frac{2}{L_1}}, \qquad \phi_{n\max} = \sqrt{\frac{2}{L_1}}$$

By using the mode shape normalization, $(A\psi_\alpha{}^2)$ was calculated:

$$(A\psi_\alpha{}^2)_{\max} = A(\psi_m\phi_n)^2 = A\frac{2}{L_1L_2} = 2 \quad (5)$$

where A was the blade surface area and the mode shapes were

α = (m, n) = (1,1), (1,2), (2,1), (2,2).

Substituting (5) into (1) resulted in further simplification of equation (1):

$$< y_\alpha{}^2(\underline{x}) >= \frac{2G_p(f_\alpha)\underline{J}_{\alpha\alpha}(f_\alpha)}{64\pi^3 m_\alpha{}^2 f_\alpha{}^3 \xi_\alpha} \quad (6)$$

The generalized mass for all the modes was only the surface mass density that was expressed by the following equation:

$$m_{mn} = \rho_m wt \quad (7)$$

The natural frequencies were calculated using the formula from Blevins [2]

$$f_{mn} = \frac{\lambda_{mn}^{\ 2}}{2\pi L_1^{\ 2}}\left[\frac{Ewt^3}{12\rho_m wt(1-\upsilon^2)}\right]^{\frac{1}{2}} \quad (8)$$

Using equation (8) and, the natural frequencies for the first four modes were found to be:

f_{11} =150 Hz, f_{12} = 782 Hz

f_{21} = 937 Hz, f_{22} = 2500 Hz

It was confirmed that the natural frequencies for, at least the first four modes, were reasonably well separated.

To arrive with the correct joint acceptance values, it was necessary to determine the boundary layer thickness and convective velocities for each mode. Streeter [3] defined the displacement boundary layer thickness as:

$$\delta^* = \frac{0.37x}{\mathrm{Re}^{\frac{1}{5}}} \quad (9)$$

which depended on Reynolds number

$$\mathrm{Re} = \frac{Vx}{\upsilon} \quad (10)$$

For the internal channel flow, the characteristic length is equal to half the channel height, see Figure 7. Therefore, the Reynolds number was expressed as:

$$\mathrm{Re} = \frac{hV}{\upsilon} \quad (11)$$

The channel dimensions, velocity, and viscosity determined the Reynolds number which exceeded value 10^6. The boundary layer thickness $\boldsymbol{\delta^*}$ was determined from the plots based on experimental results carried out by Duncan et al. in 1960. Based on the chart, the **n** value was approximately 10. Hence, δ^* was readily calculated using the following equation:

$$\delta^* = \frac{h}{n+1} \quad (12)$$

Next, the delta parameters were calculated:

$$\Delta^*_1 = \frac{\delta^*}{L_1}, \qquad \Delta^*_2 = \frac{\delta^*}{L_2} \quad (13)$$

The convective velocity was determined by using Bull's equation given in [4]:

$$U_c = V(0.59 + 0.3e^{-0.89(2\pi f)\delta^*/v}) \quad (14)$$

Knowing the convective velocity U_c; the $4fL_1/U_c$, and $4fL_2/U_c$ dimensionless parameters expressed as functions of modal frequencies were calculated. Using these parameters, the longitudinal and lateral joint acceptances for each vibration mode were read off the charts.

Next step involved the calculation of dimensionless frequency that was used to determine the normalized fluctuating pressure power spectral density ($PSD_{Normalized}$).

The dimensionless frequency was given by:

$$F_{norm} = \frac{\omega\delta^*}{V} \quad (15)$$

and the normalized PSD was determined. $G_p(f)$, the random pulsating pressure PSD, was obtained from:

$$G_p(f) = 2\pi\rho^2 V^3 \delta^* (PSD_{Normalized}) \quad (16)$$

Having determined all variables of equation (1), the mean square response for each mode of the blade was computed. From these, the modal vibratory RMS responses were obtained.

The results of this study can be found in Table 2 for the blade exposed to the original average gas velocity of 320 m/s ($\dot{V}$= 15.5 m^3 /s). The same calculations were repeated for the increased average gas velocity of 350 m/s($\dot{V}$= 17.0 m^3 /s for upgraded turbine), see Table 3.

DISCUSSION

In cases when the flow parallel to the disk-blades randomly excites the vibration modes, the transfer function and the acceptance integral can be used to evaluate the response of the disk-blade to turbulent flows. This approach could be critical for determining the integrity and fatigue life of a disk-blade. In principle, the transfer function and the acceptance integral are very similar expressions.

They both play roles in the description of a structure's response. The transfer function is a measure of matching, in time domain, the periodicity of the forcing function and the natural period of structure vibration. The acceptance integral is a measure of matching, in space, the forcing function with the structural mode shape; see Figure 4. For a point mass spring system excited by a random forcing function, the acceptance integral reduces to unity.

Only a significant frequency change in either acoustic excitation or in structural system can eliminate coupling and vibratory amplification. Sufficient frequency mode separation is estimated to be from 10% to 25%.

Calculations of the blade response presented in this work provide insight into the disk-blade behaviour and clarify directions for future designs. The evaluated responses, given in Tables 2 and 3, clearly show that an increase in flow by about 8 % noticeably changed responses in different modes, accentuating the mode (1, 2) at 782 Hz. The vibratory response of this mode was increased by 19.6%. Other modal responses were increased by 2.1% for mode (1, 1), 15.9% for mode (2, 1) and 7.2% for mode (2, 2), respectively. The predictions showed that increasing flow rate through the turbine, to gain additional power, drastically changed the modal blade-disk responses. Only flow turbulence influence has been shown in the calculations. In addition to the turbulence, there were eight combustor cans see Figure 6, which, by design, harmonically excited the blades at certain speed range. For example, the speed of 5800 rpm to 6000 rpm additionally excited the blade mode of 782 Hz in a harmonic fashion. Therefore to obtain the complete response of the turbine blade-disk at this particular mode, the turbulence, harmonic, and vortex excitations would have to be added together. Furthermore, to obtain the global vibratory disk-blade response, all of the modal responses would have to be summarized. The predictions here are not complete but still point to a potential problem which can be identified and analyzed before implementation of the turbine upgrade; for example, the modes most responsive to the flow increase can be identified and vibration caused by them quantified in a reasonable manner. Other factors could be analyzed later when the vibration increase in the identified modes is addressed.

The blade natural frequency predictions were verified by modal analysis and have surprisingly small errors, 1.3% to 12% (for the first four modes), see Table 1. The blade-channel model was sensitive primarily to the blade length and location of its anchor point, thus, special care was taken to measure the length of the blade to the actual anchor point in the middle of the fir-tree connection. The chosen length and average blade thickness well represent the blade dynamics.

The advantage of this type of analysis lays not so much in the natural frequency predictions as in the determination of the blade vibration levels. The predicted vibrations are directly related to the flow rate through the blade-channel and to the mode shape of the vibrating blade. The responses ranged from 29.1 mm/s RMS vibration velocity for the second vibration mode (1, 2) to 3 mm/s RMS for the fourth vibration (2,2) when flow was increased. As vibration measurements of disk-blade rotors in industrial service are very costly, and in most cases, even impossible to be carried out, the option of predicting responses with confidence is of great practical value. Vibration levels predicted in this work are within reasonable bounds for the frequency ranges encountered in industrial turbine disks.

CONCLUSIONS

1) Many complex excitations are present in the power turbine combustors and rotors. Higher order acoustic waves are potentially most efficient and destructive mechanisms causing disk-blade failures in turbines.
2) Whether the excitation damages the disk-blade rotor or not, depends on the coincidence between the excitation and the structural response. A full coincidence is harmful and a partial coincidence is usually safe. The transfer function and acceptance integral determine the efficiency of a coincidence for cases when flow excitations are considered.
3) The simple blade-channel model clearly shows significant vibration of the blade, for mode (1, 2) response. At other modes, the absence of an efficient coupling results in the reduction of the vibratory response. In addition, the higher frequency modes have the lower vibration levels due to 'frequency damping'.

4) Failure free design of the disk-blade is accomplished when the acoustic and structural mode shapes and their excitation frequencies do not match. Simplified calculations can provide a designer with information of the dynamic blade loading, thus point out to the critical design flaws. The blade-channel analysis determines response sensitivity of the blade to the volume flow changes.

REFERENCES

1) Au-Yang, M.K.,2000, The Joint and Cross Acceptances in Cross-Flow Induced Vibration, Part I - Theory and Part II –Charts and Applications' ASME Transaction, Journal of Pressure Vessel Technology, Vol. 122, pp. 349-361.
2) Blevins, R.D, 1979, 'Formulas for Natural Frequency and Mode shape', Van Nostrand Reinhold, New York
3) Streeter, V.L., 1966, Fluid Mechanics, Fourth Edition, McGraw Hill, New York
4) Bull, M.K., 1967, 'Wall Pressure Associated with Subsonic Turbulent Boundary layer Flow', Journal of Fluid Mechanics, vol. 28, part 4, pp. 719-754

FIGURES

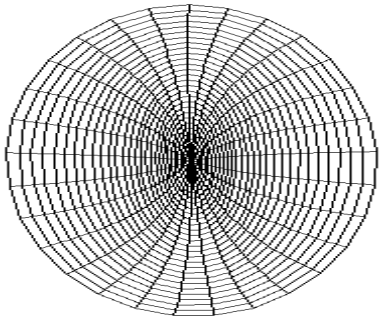

Figure 1: Acoustical Mode m= 1, n = 0, EDI

Figure 2: Example of Turbine Blade 'fir-tree' Attachment

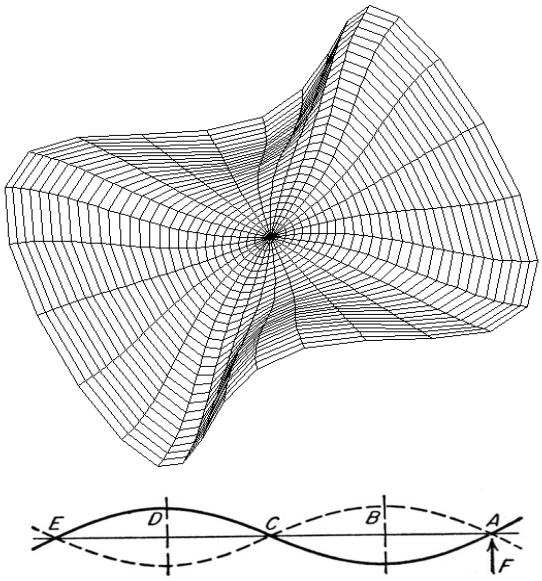

Figure 3: Three Nodal Vibration Pattern – Mode (3,0), EDI

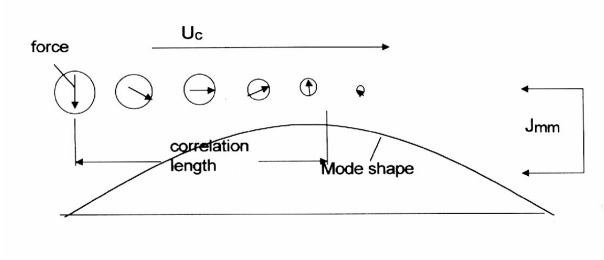

a)Joint Acceptance Representation

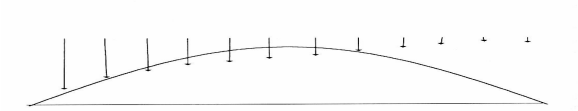

b) Symmetric Mode Excitation

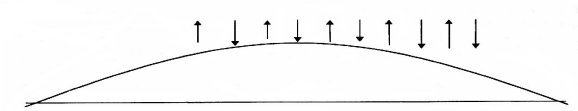

c) Non-Symmetric Mode Excitation

Figure 4: Acceptance Integral as a Compatibility Measure of Excitation and Structural Response

Figure 5: Power Turbine Blade Used in Calculations

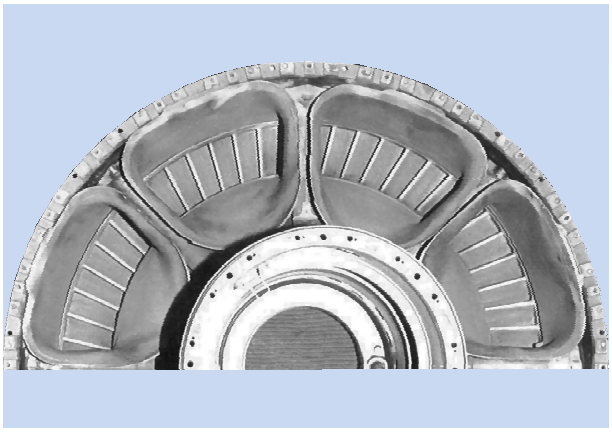

Figure 6: Power Turbine Blades - Parts Exposed to the Combustion Gas

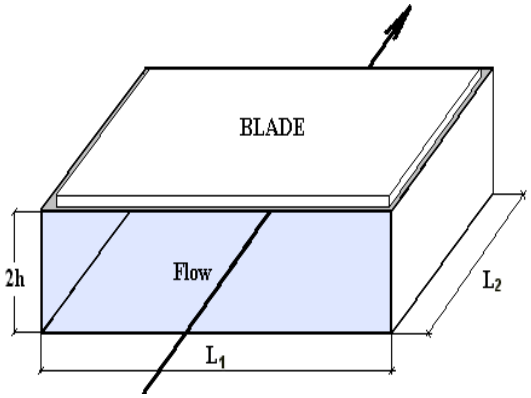

Figure7: Flow Channel with the Blade Exposed to Excitation

TABLES

Table 1: Verification of the Predicted Blade Modes

Mode	Predicted	Measured	Difference
(1,1)	150 Hz	152 Hz	1.3%
(1,2)	782 Hz	688 Hz	12%
(2,1)	937 Hz	920 Hz	9.8%
(2,2)	2500 Hz	2304 Hz	7.8 %

Table 2: Dimensions, Flow Data, and Results (before power upgrade)

Modelled Blade (48 Blades)			Nominal Blade Thickness	Exposed Blade Area	Channel Flow Area
L_1 [m]	L_2 [m]	Y [m]	[m]	[m^2]	[m^2]
0.034	0.047	0.022	0.0031	0.0016	0.0010

Actual Average Flow [m^3/s]	Gas Density [kg/m^3] Dimensions	Young's Modulus [Pa]	Poisson Ratio [1]
15.5	1.8	$2*10^{11}$	0.3

Mode [Hz]	U_c [m/s]	$4fL_1/U_c$	$4fL_2/U_c$
(1,1) 150	284.6	0.072	0.099
(1,2) 782	283.5	0.375	0.521
(2,1) 937	208.3	0.612	0.849
(2,2) 2500	190.2	1.788	2.482

Mode [Hz]	J_{mm}	J'_{mm}	$\omega\delta^*/V$
(1,1) 150	0.53	0.28	0.0029
(1,2) 782	0.52	0.27	0.0149
(2,1) 937	0.51	0.26	0.0179
(2,2) 2500	0.24	0.02	0.0478

Mode [Hz]	Norm. PSD	G_p [Pa^2/Hz]	Y^2_{RMS} [m]
(1,1) 150	$9.06\ 10^{-5}$	58.79	$3.103\ 10^{-11}$
(1,2) 782	$9.47\ 10^{-5}$	61.45	$2.258\ 10^{-11}$
(2,1) 937	$9.46\ 10^{-5}$	61.42	$1.292\ 10^{-11}$
(2,2) 2500	$9.22\ 10^{-6}$	5.98	$3.118\ 10^{-14}$

Table 3: Dimensions, Flow Data, and Results (after power upgrade)

Modelled Blade (48 Blades)			Nominal Blade Thickness	Exposed Blade Area	Channel Flow Area
L_1 [m]	L_2 [m]	Y [m]	[m]	[m^2]	[m^2]
0.034	0.047	0.022	0.0031	0.0016	0.0010

Actual Average Flow [m^3/s]	Gas Density [kg/m^3] Dimensions	Young's Modulus [Pa]	Poisson Ratio [1]
17.0	1.8	$2*10^{11}$	0.3

Mode [Hz]	U_c [m/s]	$4fL_1/U_c$	$4fL_2/U_c$
(1,1) 150	311.3	0.066	0.091
(1,2) 782	310.2	0.343	0.476
(2,1) 937	309.9	0.411	0.571
(2,2) 2500	307.5	1.106	1.535

Mode [Hz]	J_{mm}	J'_{mm}	$\omega\delta^*/V$
(1,1) 150	0.54	0.27	0.0026
(1,2) 782	0.56	0.25	0.0140
(2,1) 937	0.53	0.24	0.0164
(2,2) 2500	0.50	0.06	0.0440

Mode [Hz]	Norm. PSD	G_p [Pa^2/Hz]	Y^2_{RMS} [m]
(1,1) 150	$9.08\ 10^{-5}$	84.05	$3.220\ 10^{-11}$
(1,2) 782	$9.50\ 10^{-5}$	87.99	$3.496\ 10^{-11}$
(2,1) 937	$9.27\ 10^{-5}$	85.86	$1.877\ 10^{-11}$
(2,2) 2500	$9.34\ 10^{-5}$	8.65	$3.625\ 10^{-14}$